Spin Coating Cellulose Derivatives on Quartz Crystal Microbalance Plates to Obtain Hydrogel-Based Fast Sensors and Actuators

A. Sannino,[1] S. Pappadà,[1] L. Giotta,[2] L. Valli,[1] A. Maffezzoli[1]

[1]*Department of Innovation Engineering, University of Lecce, via per Monteroni 73100 Lecce, Italy*
[2]*Department of Materials Science, University of Lecce, via per Monteroni 73100 Lecce, Italy*

Received 22 March 2006; accepted 28 September 2006
DOI 10.1002/app.25899
Published online 13 August 2007 in Wiley InterScience (www.interscience.wiley.com).

ABSTRACT: Cellulose based superabsorbent hydrogels were spin coated and chemically crosslinked on Quartz Crystal Microbalance plates to obtain a thin superabsorbent layer. The hydrogel network was obtained by crosslinking hydroxiethylcellulose (HEC) and Carboxymethylcellulose (CMC) by the difunctional Divinylsulfone (DVS). The presence of the polyelectrolyte CMC was found to be responsible for the material high sorption sensitivity to changes in ionic strength and pH of the external solution, due to the Donnan type equilibrium established between the internal of the gel and the external solution. Since the hydrogel was synthesized in the form of a thin layer, there is negligible barrier to water diffusion through the material, which results in a fast swelling response to changes in the external solution properties. The device was immersed in a flux of water solution, where the ionic strength was continuously changed. The fast change in the equilibrium sorption capacity of the spin coated hydrogel were converted to an electrical signal by the apparatus. The time lag of the response was comparable to the inverse of the quartz oscillation frequency (approximately 10^{-7} s), and the accuracy in the weight change measurement was of the order of the nanogram. FTIR microscope analysis was used to determine the presence of hydrogel and its distribution on the QCM plate. © 2007 Wiley Periodicals, Inc. J Appl Polym Sci 106: 3040–3050, 2007

Key words: hydrogel; swelling; ionic strength; sensors

INTRODUCTION

Polyelectrolyte hydrogels, which display a sorption capacity in water and water solutions as high as 1 L/g of dry polymer, can be used to produce sensors and actuators, owing to their swelling sensitivity to variations of ionic strength and pH of the external solutions.

The high sensitivity of thin hydrogel layers to changes of external environment results in a high quality of the kinetic response of such a device. Recent research studies have been concerned with the enhancement of the swelling capability and response rate to external stimuli. This has been achieved by downsizing the hydrogel or by means of open microporosity within the material. The response rate can be significantly enhanced by downsizing the hydrogel since the diffusion rate is inversely proportional to the square of the characteristic length.[1–3] This approach has led to the development of microgel nanoparticles, which exhibit a very fast response to external stimuli.[4–6] Their use is currently being exploited for several applications,[7] such as drug delivery,[8–10] biosensors,[11] soft actuators/valves,[12] and catalysis.[13]

The second approach relies on the open porosity within the hydrogel to increase the surface area to volume ratio, thereby enhancing the diffusion rate of water within the material. Various methods have been developed to produce microporous hydrogels.[14–19] The use of lyotropic surfactants leads to a wide variety of morphologies, such as layerlike architectures, ''cauliflower'' structures, and gel sheets or platelets with a pore size spanning from hundreds of nanometers to micrometers depending on the type of monomers and surfactants used. Ikada et al.[20] showed that by using freeze-drying it is possible to obtain a controlled open porosity. Other techniques are based on the segregation of the solvent from the polymer network during the polymerization process.[21] Chen et al.[22–24] have developed a *bubbling* technique to obtain an open porosity within polymer gels based on the entrapment of CO_2 bubbles within the polymer network during its formation. The entrapment of the CO_2 gas is obtained by finely adjusting the bubbling time to the gelation time. In this way it is possible to modulate both pore size and structure by fine tuning these two variables. Porous hydrogels show high swelling capacity and faster swelling kinetics when compared to solid hydrogels.

Correspondence to: A. Sannino (alessandro.sannino@unile.it).

Journal of Applied Polymer Science, Vol. 106, 3040–3050 (2007)

However, the large majority of swelling kinetic studies on hydrogels have been performed gravimetrically,[25–29] which does not lend itself to closely monitor the rapid mass changes when the external environment conditions are changed. The piezoelectric quartz crystal microbalance system (PQCM), in turn, allows an on-line monitoring of the hydrogel mass change to be implemented, thus providing a good measurement accuracy.

Biodegradable and organic materials are used as chemical or physical layers for many applications in modern sensors and actuators.[30–33] In particular, when a chemical reaction takes place at the surface of a sensor, there is a change of mass, which can be converted into an electrical signal by piezoelectric quartzes.

The QCM sensor used for our measurements consists of a thin quartz disc with circular electrodes on the lower side of the quartz. This is known as ''one-side cell.'' In this system the contact with the solutions is circumscribed only to one face of the quartz crystal, to decrease the extent of liquid damping and getting rid of effects connected to conductivity and dielectric constant.[34] Because of the piezoelectric properties of quartz, a voltage between these electrodes leads to a shear deformation of the constituent crystal. Sauerbrey et al.[35] have described the relation between a mass deposition on the quartz surface and the resulting shift in the fundamental oscillation frequency of the quartz. If a physical or chemical layer exists on the upper surface of the quartz, the resonance frequency of the quartz decreases proportionally to the number of absorbed molecules, so that a mass change of the layer on the crystal can be measured in terms of changes in frequency.

With the view to obtain sensors or actuators device with a fast response to changes in the external solution characteristics, a thin layer of polyelectrolyte hydrogel was deposited on the surface of quartz plate by spin coating. When the water solution contacts the sensing element, the gel absorbs water and increases its mass: frequency change is thus observed, and correlated to the hydrogel mass change. To verify the principle, the solution ionic strength was changed several times, from low to high values, to observe the signal variations of the designed apparatus. Fast responses to changes in external solution ionic strength changes were always observed, and a final accurate value of the weight variation was also obtained.

Moreover, the proposed technique makes it possible to perform kinetic studies on hydrogel performances following the experiments all through their length, without the need to carry out any gravimetrical measurements, thus reducing the errors related to the periodically removing of samples from its location.

In this study cellulose polyelectrolyte-based hydrogels chemically crosslinked with divinylsulfone were used.

EXPERIMENTAL

Materials

Cellulose based hydrogels were prepared using aqueous solution mixtures of carboxymethylecellulose sodium salt (CMCNa) and hydroxyethylcellulose (HEC), crosslinked with the use of divinylsulphone (DVS). CMCNa and HEC are both cellulose ethers, where the substituent groups are methylcarboxylic groups and oxyethylene chains respectively, (Fig. 1). The degree of substitution and the relative distribution of substituents in C-2, C-3, and C-6 position has a large affect on the equilibrium sorption properties of these polymers.

CMCNa, HEC, and DVS were purchased from Aldrich Chimica s.r.l. Milano and were used as received.

The NaCl for tests at different ionic strength and the KOH used as a catalyst were also purchased from Aldrich, Milano.

Hydrogel production

The materials investigated in this work were obtained by chemical crosslinking of carboxymethylcellulose sodium salt (CMCNa) and hydroxyethylcellulose (HEC) stabilized in a 3-D network. The procedure for the preparation of hydrogels at low polymer concentrations, together with the analysis of the degree of crosslinking of the polymer network, has been reported elsewhere.[36,37] According to this procedure, the reaction is performed in an aqueous solution at 2% polymer concentration by weight (CMCNa/HEC weight ratio 3/1). Divinylsulfone (DVS) is added to the solution as a crosslinking agent at a concentration equal to 0.04*M*. After complete mixing, KOH is added to the solution as a catalyst at concentrations up to a 0.02*M*. The crosslinking reaction begins when the solution viscosity rapidly increases and it takes place in approximately 24 h. Since the products consist of

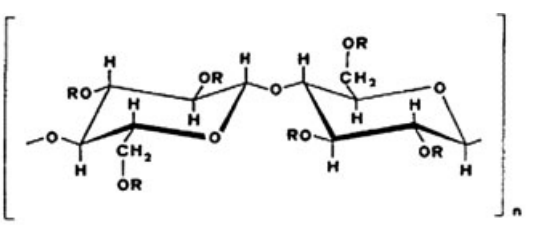

cellulose derivatives

CMCNa R= -H, -CH_2COONa
HEC R= -H, CH_2CH_2OH,
- CH_2CH_2O CH_2CH_2OH,
- CH_2CH_2O CH_2CH_2O CH_2CH_2O CH_2CH_2OH

Figure 1 CMCNa.

partially swollen gels, a purification procedure is required to remove from the hydrogel the KOH, the unreacted DVS, and all the other impurities. Purification is carried out by washing the material several times in distilled water, until the equilibrium sorption capacity is reached (i.e., until the sample weight remains constant). Finally, the hydrogel is desiccated in air at room temperature.

Hydrogel deposition on the quartz plate

The spin coating apparatus consists of a rotor with a hole on its upper surface connected to an air-pump. The quartz is positioned on the hole so that when the air-pump is turned on the quartz sticks to the rotor. Thus, a drop of the hydrogel precursor solution (before the KOH catalyst addition to the polymer-DVS solution) is placed on the quartz, and the rotor is turned on for thirty seconds at 4000 rpm to cover the entire quartz surface as a thin layer. Since at this stage, the gel is still uncrosslinked, the crosslinking catalyst is placed on the hydrogel precursor solution covering the quartz surface. The quartz is thus stored in a covered humidity box for 24 h, to allow crosslinking to be completed and to prevent the desiccation of gel layer. After the crosslinking reaction has taken place, the resulting hydrogel is washed while on the quartz plate, and it is then desiccated in air atmosphere at room temperature.

FTIR measurements

FTIR measurements were performed using a PerkinElmer Spectrum One mid-IR spectrometer equipped with a TGS detector. For FTIR microscopy a Spotlight microscope accessory (PerkinElmer) equipped with a multiarray MCT detector was attached to the FTIR spectrometer. The hydrogel coated quartz crystals were placed on a computer controlled motorized stage, which was set to move in the x-y plane with a step of 25 μm. At each position in the two-dimensional grid 8 interferograms were averaged at a resolution of 4 cm^{-1} per each spectrum with an aperture able to cover a cross-sectional area equal to 25 × 25 μm^2. The spectra were recorded in reflection modality and rationed against a background collected on a bare quartz crystal surface.

Infrared spectra of CMCNa and HEC were recorded by means of an horizontal ATR-accessory (SensIR technology). The IRE was a 3 mm diameter three-reflection diamond microprism. In order that the sample could be made to adhere to the prism surface an aqueous cellulose suspension was placed on the ATR crystal and the solvent was allowed to evaporate. The spectra of the dried polymer were acquired at 4 cm^{-1} resolution and 8 interferograms were accumulated and averaged for each trace.

The "Liquilab" apparatus

A lay-out of the quartz device is reported in Figure 2. Crystals consists of 1 cm diameter dishes and have the contacts on their lower surface, while the upper surface is covered with a gold layer. The quartz used for the measurements has a constant equal to 82,379 × 10^{-9} g/Hz, that is a frequency change of 1 Hz corresponds to a mass change equal to 82,379 × 10^{-9} g. A photograph of the measurement cell is reported in Figure 3. The quartz crystals are immersed in water or water solutions and rubber tubes are used to establish the water flux. A frequency transducer is positioned on the bottom of the apparatus. The quartz is fixed in the cell by means of two *o*-rings, one in the upper face and one in the lower face.

The water flux is obtained by means of a peristaltic pump. A picture of the measurement device is reported in Figure 4. The experimental set-up is assembled in a modular structure, which allows a specific adaptation on user requirements. All system components are arranged in a thermostatic box. Control of the set-up and data visualization, as well as data storage, are performed by dedicated software. The measurement device is produced and distributed by "Liquilab."

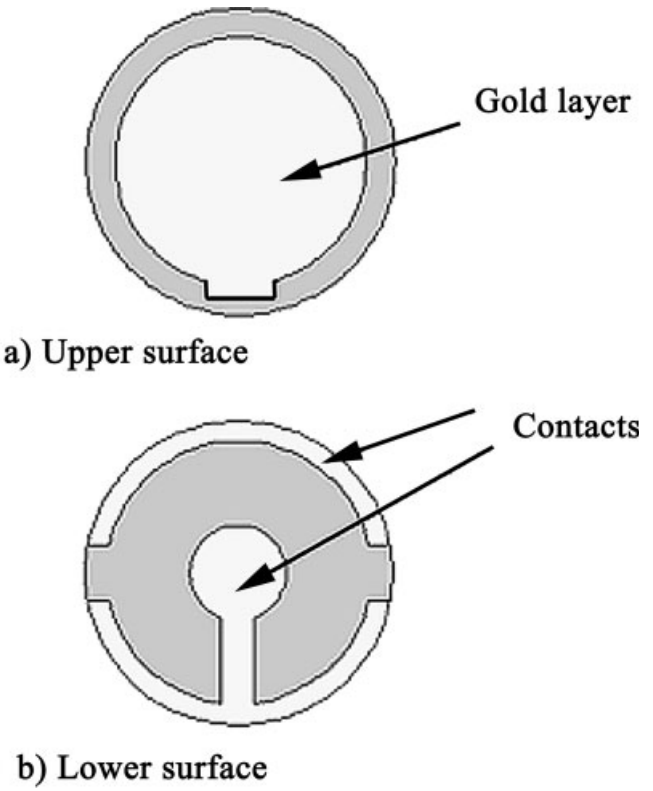

Figure 2 Images of the quartzes used in the measures.

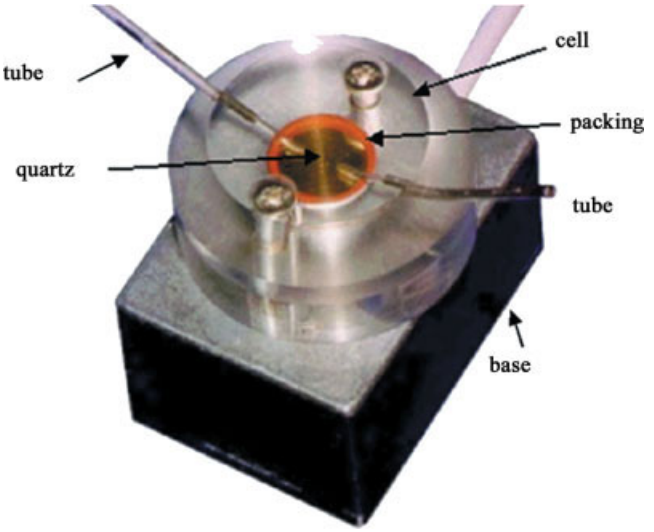

Figure 3 The cell of Liquilab 21. [Color figure can be viewed in the online issue, which is available at www.interscience.wiley.com.]

RESULTS AND DISCUSSION

Hydrogel deposition analysis

To perform the QCM measurements, the apparatus chamber was first filled with distilled water, and a constant water flux was maintained in the chamber to allow the hydrogel to reach the equilibrium sorption value. At this stage the hydrogel is also purified from all impurities, such as unreacted DVS, KOH catalyst, and traces of uncrosslinked CMCNa and HEC.

After equilibrium swelling was reached, the ionic strength of the water solution flux was increased slightly by adding increasing amounts of NaCl. Simultaneously, the same water solution change was performed in a second measuring chamber, in which was placed the same

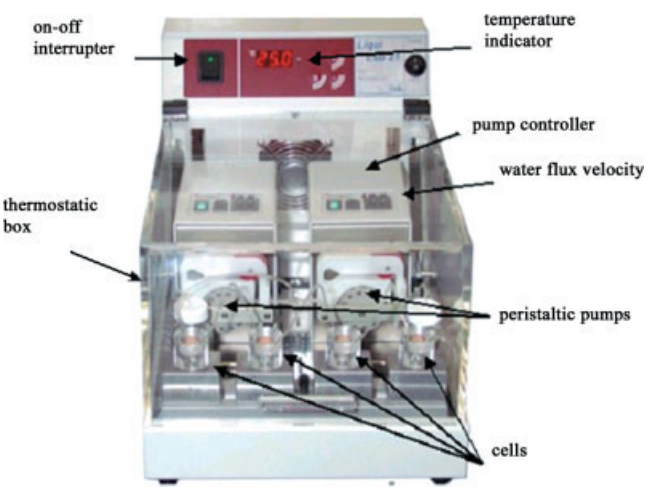

Figure 4 Liquilab 21 apparatus. [Color figure can be viewed in the online issue, which is available at www.interscience.wiley.com.]

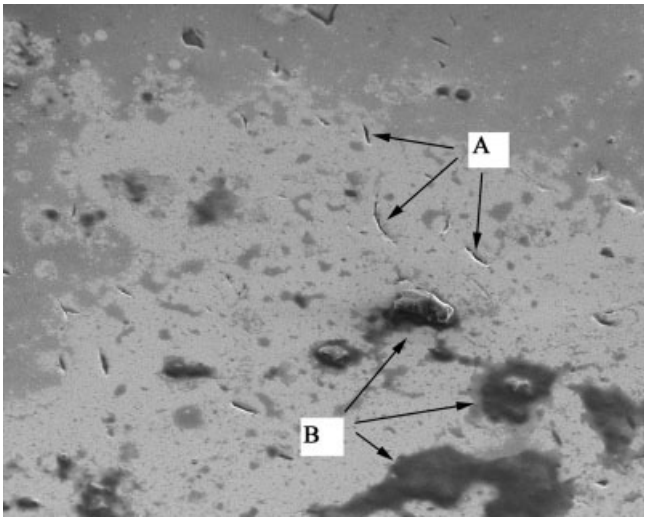

Figure 5 Image of the not yet crosslinked gel after deposition on the quartz plate (×2000, accel. volt. 3 kV, WD 7.7).

quartz crystal, without any gel positioned on it. In such a way it is possible to know the frequency change due to the change of liquid properties.

A morphological examination of the hydrogel film deposited on the quartz crystals was performed by means of scanning electron microscopy (SEM).

A SEM micrograph of the hydrogel film deposited on the quartz crystal before the crosslinking reaction is reported in Figure 5.

The layer shows a reasonably uniform thickness, even though some gel accumulation has taken place in specimens (see ''B'' arrows). Formation of cracks have also been observed after deposition (see label A).

Micrographs performed after crosslinking reaction does not show any significant difference in hydrogel distribution (see Fig. 6).

Figure 7 shows a micrograph of the dry gel after washing in distilled water. The quartz was immersed in water and then kept in air for 24 h to desiccate the gel. Regions in which the gel thickens, forming lumps (see A arrows), are visible together with areas in which (see B arrows). C arrows show the straight lines probably caused by the crystal substrate of quartz, while D arrows indicate the advancing lines of the gel during the spin coating. However, a predominantly uniform hydrogel distribution was observed on quartz crystal in the configuration preceding the sorption test.

Further information about chemical composition and morphology of the spun layers was acquired on a bigger scale by FTIR spectroscopy. Figure 8(a,c) show the visible image of a 4×4 mm^2 area of the hydrogel coated quartz surface, respectively, as prepared and after perfusion with pure water. The two areas do not coincide perfectly due to the difficulty in placing the round-shaped crystal in the same position and with the same orientation on the microscope stage, after

removing it for washing. Nevertheless it is clear that a correspondence higher than 80% exists between the pixels scanned before and after the treatment. Using a 25 μm step an infrared map represented by 161 × 161 spectra for the selected area was acquired. The two spectra obtained averaging the resulting 25,921 infrared spectra acquired before and after water perfusion are shown in Figure 9. CMC signals are particularly evident in both traces consistently with the higher percent of this component in the mixed hydrogel. The ATR-FTIR spectrum of CMCNa is reported in Figure 10 for comparison. It shows characteristic cellulose peaks around 1000–1200 cm^{-1}, arising from the ether C—O—C stretching vibrations, while the band around 1410 cm^{-1} is ascribable to CH_2 bending modes. The bands near 3400 cm^{-1} are representative of O—H stretching vibrations while two absorption signals at 1591 and 1325 cm^{-1} are associated to asymmetric and symmetric stretching of COO^- groups. The two spectra in Figure 9 look like merely differently scaled versions of the same spectrum except for the slight shoulder around 1650 cm^{-1}. This indicates that the hydrogel chemical composition does not change owing to the perfusion treatment except for some slight decrease in water content, responsible for the band at 1650 cm^{-1} (bending mode).

Even though reflection spectra should be used with caution for quantitative analysis, especially when both specular and diffuse reflectance account for the signals recorded, the different intensities of bands in these traces reveal that a loss of sample occurred during the washing procedure. The single wavenumber two-dimensional maps, shown in Figures 8 (b,d), also demonstrate that some hydrogel was lost when the sample was perfused with pure water. These maps were obtained by plotting the intensity of the absorption at 1596 cm^{-1} over the scanned surface, using

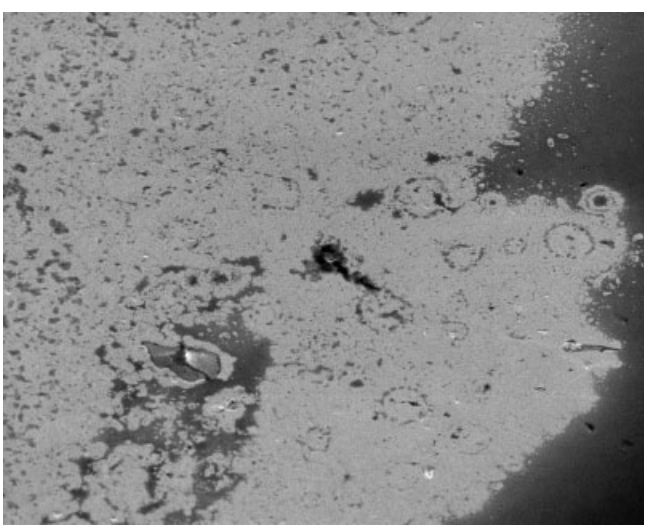

Figure 6 Image of the humid crosslinked gel on the quartz plate (×8500, accel. Volt. 5 kV, WD 8.7).

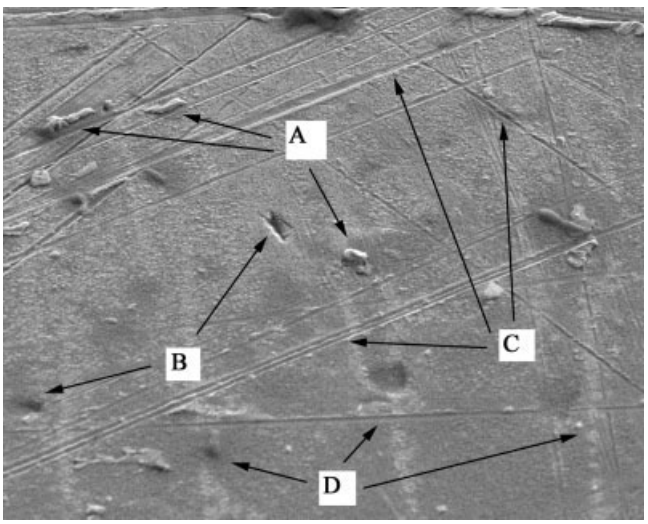

Figure 7 Image of dry crosslinked gel on the quartz plate (×10,000 accel. volt. 5 kV, WD 7.8).

1848 cm^{-1} as a reference wavenumber. Image statistics has made it possible to determine that the percent of pixels associated with absorption values at 1596 cm^{-1}, above 0.5 absorbance units, was 7.0. After the washing procedure this value dropped down to 3.4. Moreover these single wavenumber two-dimensional plots reveal that shrinking of the polymer during the drying process results in the formation of domains over the surface. The mean diameter of these polymer rich regions ranges from 0.1 to 2 mm. A three-dimensional surface projection of the region selected in Figure 8(d) is presented in (e) showing one of these domains. Apart these highly concentrated regions the remaining area appears homogenously covered by a thin hydrogel layer giving rise to an IR absorption at 1596 cm^{-1} below 0.05 absorbance units.

Equilibrium swelling measurements

Before starting the swelling kinetic measurements, the equilibrium sorption capacity of the hydrogel was measured for each of the selected values of the solution ionic strength.

The equilibrium sorption capacity was then assessed as the asymptotic limit of the swelling kinetic curve related to each ionic strength value. Swelling equilibrium in distilled water was also measured.

The effect of ion concentration on hydrogel equilibrium swelling capacity was studied by equilibrating desiccated gel samples in solutions at different NaCl concentrations (0.01; 0.05; 0.15; and 0.5 mol/L). Samples were then weighted again after 24 h, when equilibrium swelling was reached. The water solution was periodically changed with fresh solution to remove impurities expelled from the hydrogel during the swelling. All the tests have been performed in quadruplicate. The swelling capacity was expressed in

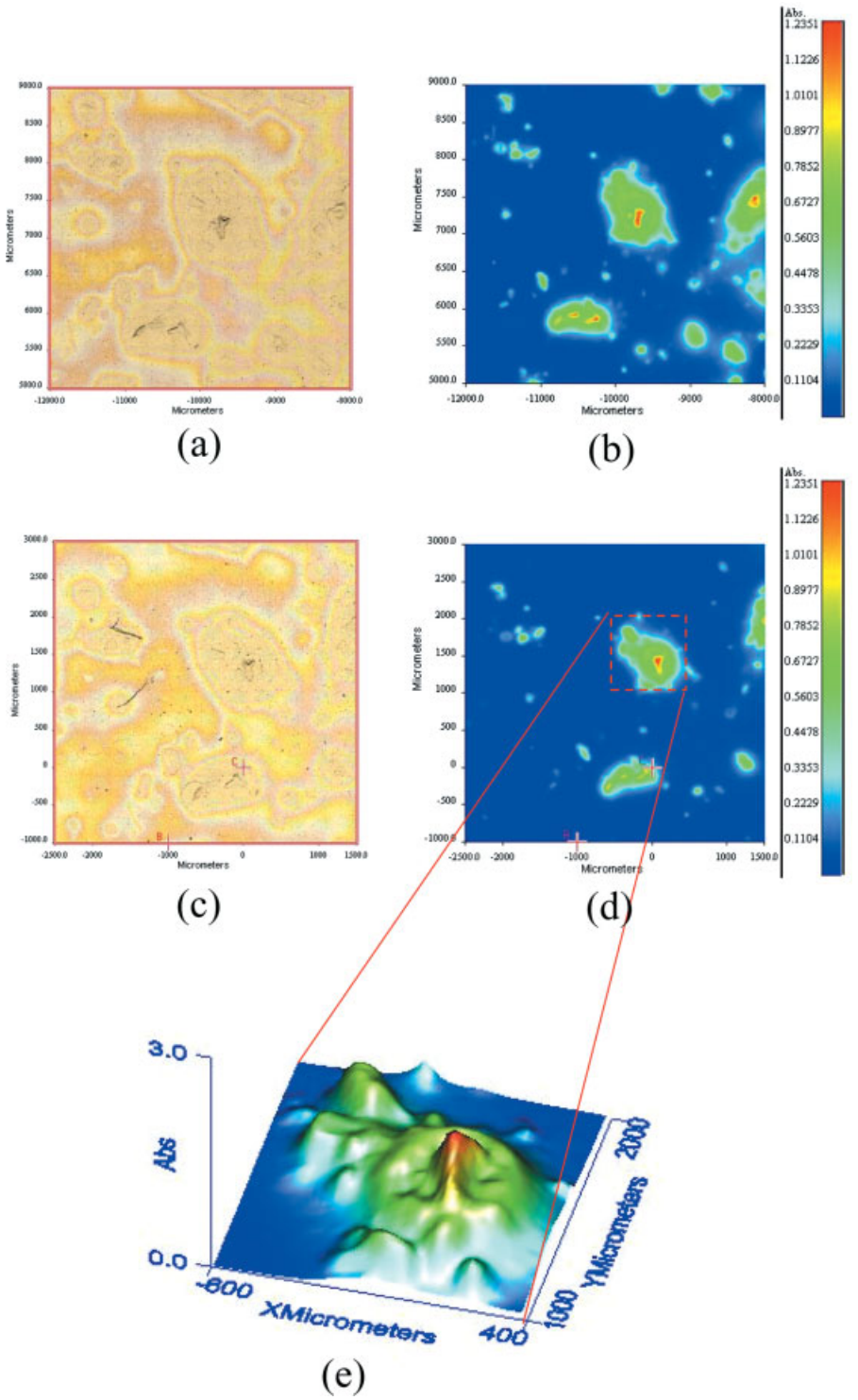

Figure 8 FTIR analysis. [Color figure can be viewed in the online issue, which is available at www.interscience.wiley.com.]

terms of swelling ratio, as:

$$\text{S.R.} = \frac{W_w - W_d}{W_d}$$

where W_w and W_d are the wet and dry sample weight, respectively.

A monotonic decrease in swell ratio was observed with increasing the ionic strength of the external solution for all the samples tested (see Fig. 11).

This behavior was related to the polyelectrolyte nature of the polymer chains, since the fixed charges on the polymer backbone is expected to play an essential role for the swelling mechanism. This is related to the

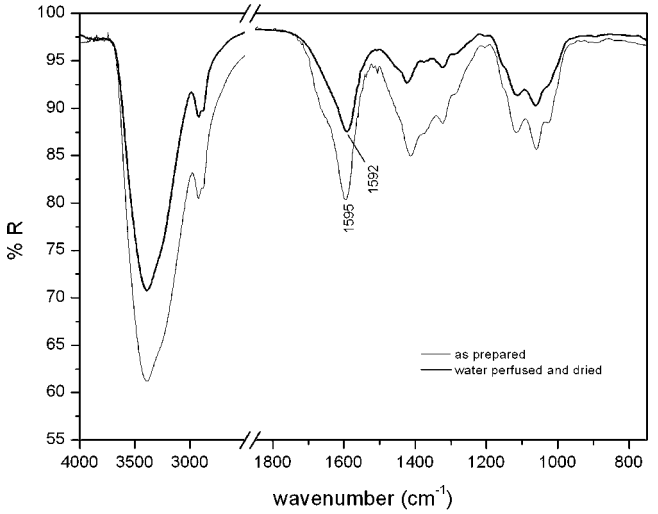

Figure 9 Spectra of the hydrogel obtained with FTIR analysis.

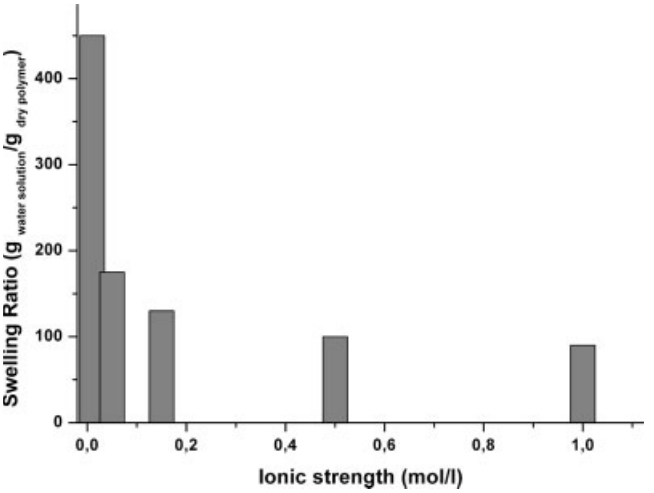

Figure 11 Swelling ratio observed increasing the ionic strength of the external solution.

electrostatic repulsion between charges of the same sign, and to the ''Donnan type'' absorption contribution to water sorption, by the generation of an osmotic pressure into the hydrogel. Both contributions to hydrogel swelling decrease with increasing the ionic strength of the solution in contact with the gel.

Kinetic measurements

The QCM working system relies on the use of a thin quartz crystal, physically or chemically sensitive to a mass change.[35,38–44]

A piezoelectric quartz crystal can be represented as a component of an electric circuit, called Butterworth–Van Dyke (BVD) circuit (see Fig. 12), having two branches. The kinetic branch represent the oscillating quartz, while the static branch represents the crystal in a static working mode. The condenser C_0 in the static branch exhibits the capacitance created by the two electrodes and associated to manufacturing defects. In the kinetic branch, the inductance L_1 is related to the mass of oscillating quartz, while the capacitance C_1 is related to the elasticity of the quartz (it is a measure of the energy stored in the crystal during each oscillation). The resistance R_1 represents the losses in the quartz, frictional or thermal, and to junction imperfections. If the quartz crystal is installed into an oscillator circuit able to exciting the quartz with an electric oscillating signal, the quartz will begin to oscillate for the inverse piezoelectric effect. At a certain frequency value, the resonance frequency, the quartz has only a resistive behavior.

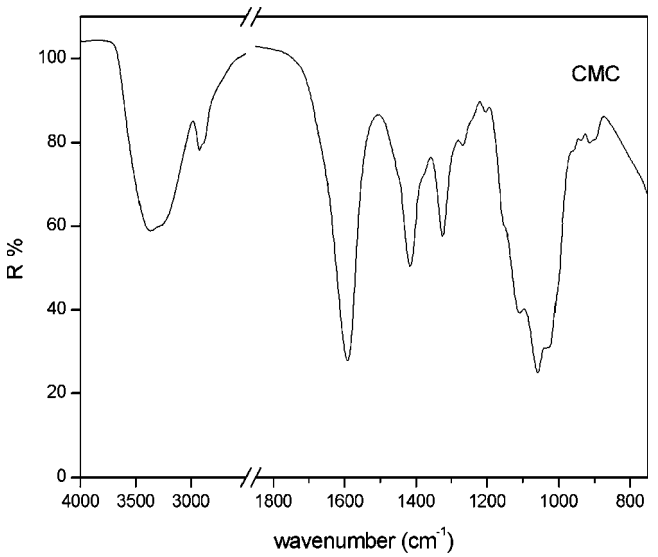

Figure 10 ATR-FTIR spectrum of CMCNa obtained with FTIR analysis.

The frequency of oscillation of a quartz crystal depends on both its total mass and the mass of the layer (or electrodes) on its surface. When some molecules are absorbed on the surface of a thin film, the resonance frequency of the quartz decreases proportionally to the number of absorbed molecules. Thus a mass change of the film on the crystal can be measured by a measurement of frequency.

The simple relationship that permits to convert a frequency variation into a mass measurement is the Sauerbrey's equation:[35]

$$\Delta f_s = -C_f \Delta m_f \tag{1}$$

where Δf_s is the change of frequency, Δm_f is the mass change and C_f is the characteristic constant of the quartz, equal to:

$$C_f = \frac{2f_0^2}{A(\rho_q \mu_q)^{1/2}} \tag{2}$$

where f_0 = the resonant frequency of the fundamental mode of oscillating of the crystal;

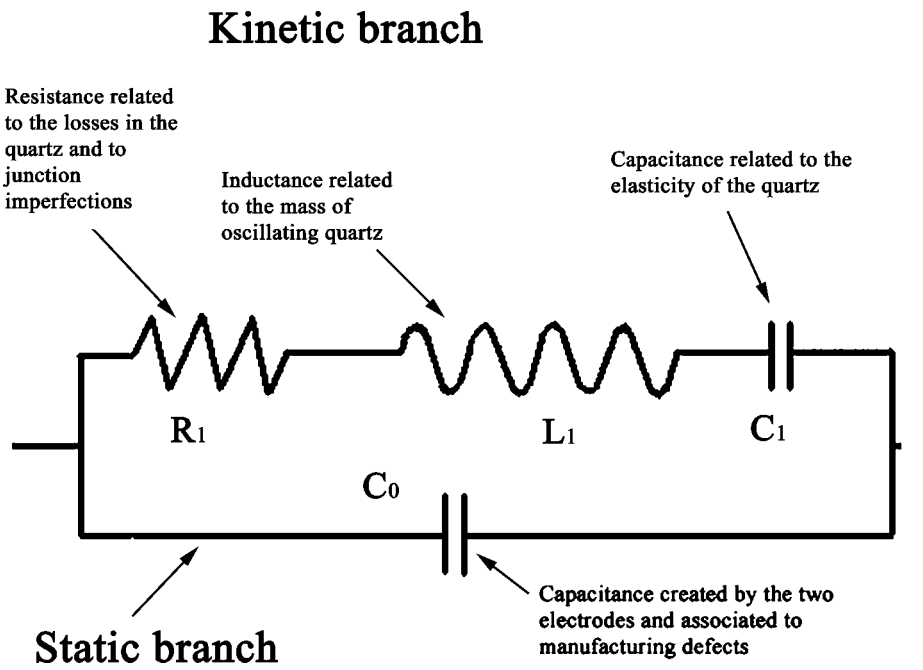

Figure 12 Equivalent circuit for a piezoelectric quartz.

A = the piezo-electrically active area;
ρ_q = the quartz density, 2648 g/cm^3;
μ_q = the quartz shear modulus, 2947 $\times$ 10^{11} g/cm s^2.

Sauerbrey's equation is valid if no appreciable changes occur to the deposited film properties. There are situations where the Sauerbrey equation does not hold. For example, when the added mass is not rigidly deposited on the electrodes surface, slips on the surface or not uniformly deposited on the electrode. Therefore, the Sauerbrey equation is only strictly applicable to uniform, rigid, thin film deposits.

A quartz crystal can be excited to a stable oscillation when it is completely immersed in a liquid. In this case, the equivalent circuit is the one represented in Figure 13, called Modified Butterworth–Van Dyke (MBVD) circuit. Some circuit components present in Figure 13 are not present in the circuit reported in Figure 12: L_m and R_m are the inductance and the resistance due to the mass effect, C_L is the capacitance related to liquid dielectric properties and the quartz electric contacts, R_L quantifies the liquid conductivity.

When a resonating crystal contacts a Newtonian liquid, the crystal effective inertia increases as the result of the vibrating crystal dragging the liquid in a narrow boundary layer near the surface. Kanazawa et al. and successive authors[42–47] have shown that the change in the resonant frequency of a QCM into a liquid is proportional to the product of the square root of the liquid density and viscosity:

$$\Delta f_D = f_u^{2/3}\left[(\rho_L \eta_L)/(\pi \times (\rho_q \mu_q))\right]^{1/2} \quad (3)$$

where:

f_u = resonant frequency of the unloaded crystal;
ρ_L = density of the liquid in contact with the crystal;
η_L = viscosity of the liquid in contact with the crystal.

Martin et al.[43] have shown from a piezomechanical model that the total frequency shift, δf_T, for simultaneous deposition and liquid damping on smooth crystals is:

$$\Delta f_T = \Delta f_S + \Delta f_D + \Delta f_X + \Delta f_A \quad (4)$$

where Δf_A is due to mechanical stress on the crystal when mounted in a liquid cell and Δf_x accounts for all

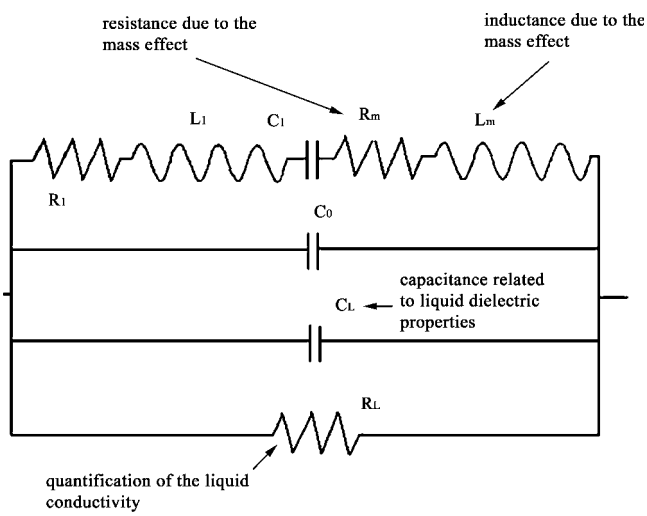

Figure 13 Equivalent circuit for a piezoelectric quartz in a liquid.

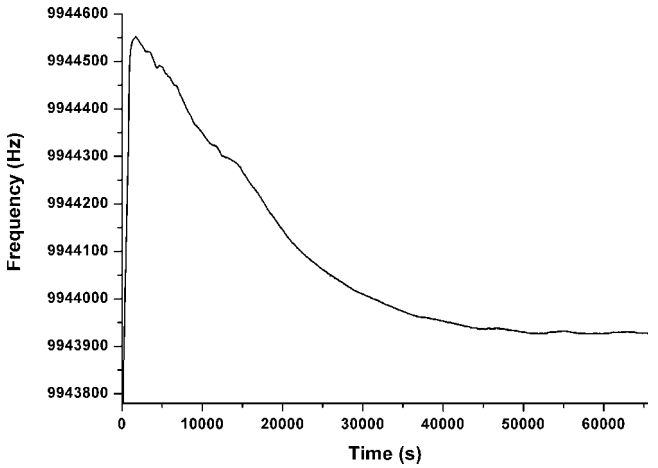

Figure 14 Frequency signal of the quartz in a measure performed using a water flux equal to 0.4 mL/s.

nonshear couplings between the liquid and the oscillating crystal.

The stress effect δf_A can be minimized by an appropriate designed cell (i.e., quartz assembly) and a carefully performed measurement. δf_X includes effects related to surface roughness and molecular-level interfacial interactions. The values that δf_X can assume are negligible in the measurements described in this work. The frequency shift δf_D is also negligible, as revealed by experiments at different values of liquid density and viscosity performed on quartzes with no hydrogel on their surface. Thus, computating the QCM test results with the Sauerbrey equation a good agreement has been obtained with the hydrogel swelling data obtained by gravimetric measurements.[36,38,48]

The first step in sorption test is the sample washing procedure, performed directly in the cell containing the quartz. To this end, the cell was filled up with water and a constant flux of 0.1 mL/s of water was established by means of a peristaltic pump.

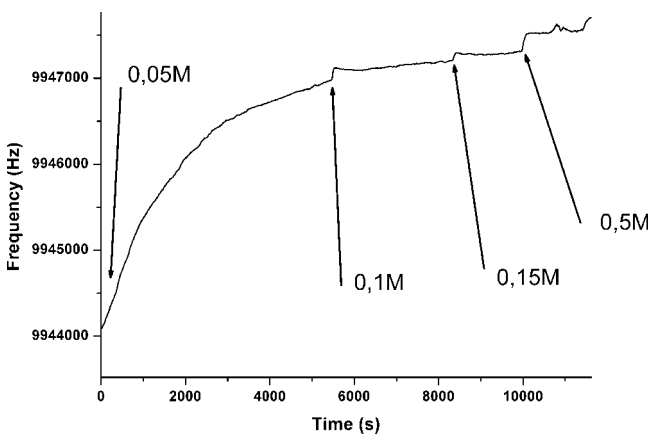

Figure 15 Frequency signal of the quartz in a measure performed in a solution where the ionic strength is increased periodically.

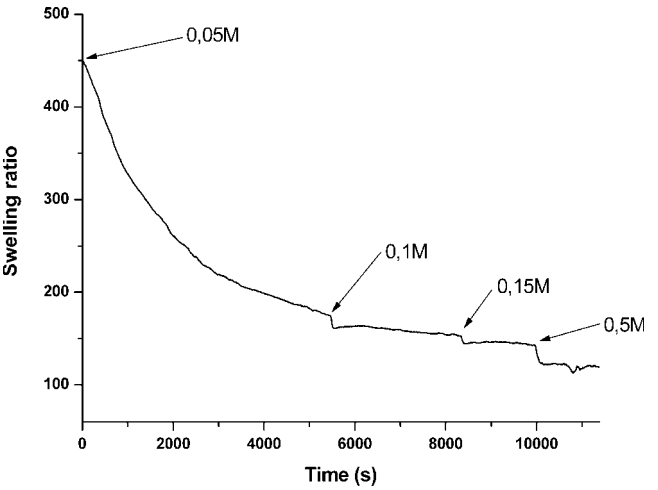

Figure 16 Hydrogel swelling ratio versus time in a measure performed in a solution where the ionic strength is increased periodically.

Under this conditions after washing for 24 h the hydrogel reached the equilibrium sorption capacity,[49,50] and impurities present in the hydrogel (such as unreacted polymer, catalyst, unreacted crosslinker), are removed. The frequency decrease is observed because of water sorption by hydrogel (see Fig. 14). At this stage, the ionic strength of the external solution is progressively changed from 0 to 0.05, 0.1, 0.15, and 0.5*M*, and frequency changes are reported in Figure 15.

The frequency increase is observed for each time interval related to the ionic strength increase, and from the frequency changes we obtained mass changes (eqs. 1 and 2). Thus, a decrease of the hydrogel sorption capacity is registered increasing the ionic strength of the external solution, as expected for a polyelectrolyte hydrogel.[48] In Figure 16 is reported a plot of the swelling kinetic at different values of ionic

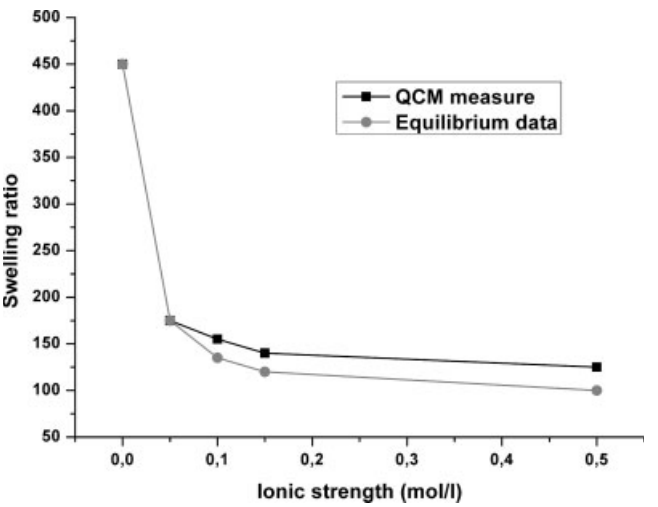

Figure 17 Comparison between the swelling data obtained in the equilibrium gravimetric swelling tests and the results obtained by means of the QCM technique.

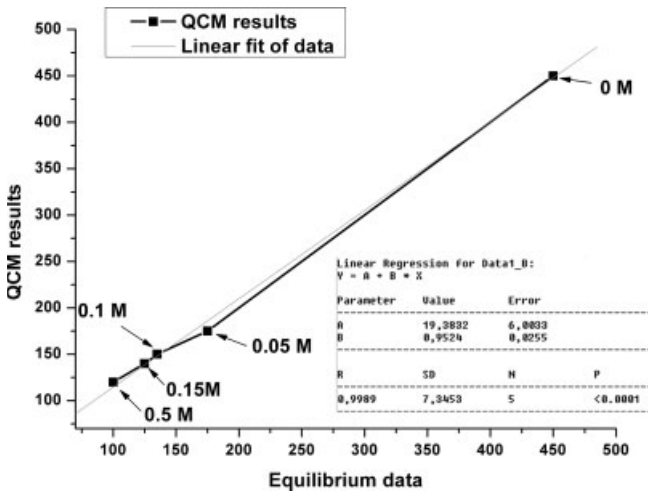

Figure 18 QCM results versus equilibrium data.

strength. The data were obtained from Sauerbrey equation (eq. 1), measuring the frequency change from the plot and evaluating the mass variation.

Equilibrium sorption capacity in correspondence of each tested value of ionic strength is reported in Figure 17. The values are reported both as evaluated from these measurements and as evaluated performing swelling tests directly on hydrogel samples immersed in solutions at different ionic strength, extracted and weighted after 24 h. In Figure 18 a plot of QCM results versus equilibrium data is reported, with the linear fit of data. A good agreement between both results was observed: the difference observed between gravimetrically and QCM measures is due to the terms δf_D, δf_X, δf_A of eq. (4): however this difference is less than 7%.

CONCLUSIONS

The possibility to produce macromolecular hydrogel based sensors and actuators has been tested in this work, crosslinking a superabsorbent polyelectrolyte on the plate of a QCM device by a spin coating procedure. The material was a cellulose based hydrogel, where network chemical stabilization was achieved using DVS as crosslinker. The analysis of the actual hydrogel deposition on the plate was performed by means of FTIR microscopy and SEM analysis. A thin hydrogel layer deposition with a uniform distribution was observed.

Being the CMC, one of the network constituents, a polyelectrolyte, the hydrogels displays a sensitivity to variations of ionic strength and pH of the water solution in which it is immersed, and the change in mass results in a change of the oscillating frequency of the quartz plate with a fast response (comparable to the inverse of the oscillation frequency, 10–7 s), and a final accuracy on the weight variation of the order of nanograms. As a proof of principle, a test was performed immersing the hydrogel coated quartz in a water solution where ionic strength was changed from low to high values. QCM output data were re-elaborated and transformed in weight change data by means of the Sauerbrey theory. To test the accuracy of this method, equilibrium swelling measurements were performed gravimetrically on the same hydrogel coated on the quartz plate, in water solution with the same ionic strength adopted for the QCM test. A good agreement between equilibrium swelling gravimetric data and the asymptotic values of the kinetic QCM measurements was achieved.

This method should be also considered as an improvement in the hydrogel swelling kinetic measurements techniques, as it allows to perform the measurements keeping the material in water, thus avoiding all the errors and the time lag related to the material extraction from the water solution and the excess water elimination procedure required.

References

1. Tanaka, T.; Fillmore, D. J. J Chem Phys 1979, 70, 1214.
2. Li, Y.; Tanaka, T. J Chem Phys 1990, 92, 1365.
3. Matsuo, E. S.; Tanaka, T. J Chem Phys 1988, 89, 1695.
4. Pelton, R. Adv Colloid Interface Sci 2000, 85, 1.
5. Wu, X.; Pelton, R. H.; Hamielec, A. E.; Woods, D. R.; McPhee, W. Colloid Polym Sci 1994, 272, 467.
6. Duracher, D.; Elaissari, A.; Pichot, C. Macromol Symp 2000, 150, 305.
7. Wang, J.; Gan, D.; Lyon, L. A.; El-Sayed, M. A. J Am Chem Soc 2001, 123, 11284.
8. Park, T. G. Biomaterials 1999, 20, 517.
9. Makino, K.; Hiyoshi, J.; Ohshima, H. Colloids Surf B 2001, 20, 341.
10. Ichikawa, H.; Fukumori, Y. J Controlled Release 2000, 63, 107.
11. Holtz, J. H.; Asher, S. A. Nature 1997, 389, 829.
12. Beebe, D. J.; Moore, J. S.; Bauer, J. M.; Yu, Q.; Liu, R. H.; Devadoss, C.; Jo, B. H. Nature 2000, 404, 588.
13. Bergbreiter, D. E.; Case, B. L.; Liu, Y.-S.; Caraway, J. W. Macromolecules 1998, 31, 6053.
14. Yan, Q.; Hoffman, A. S. Polym Commun 1995, 36, 887.
15. Kang, H.; Tabata, Y.; Ikada, Y. Biomaterials 1999, 20, 1339.
16. Appel, R.; Xu, W.; Zerda, T. W. Macromolecules 1998, 31, 5071.
17. Murphy, S. M.; Skelly, P. J.; Tighe, B. J. J Mater Chem 1992, 2, 1007.
18. Antonietti, M.; Caruso, R. A.; Goltner, C. G.; Weissenberger, M. C. Macromolecules 1999, 32, 1383.
19. Antonietti, M.; Goltner, C.; Henyze, H.-P. Langmuir 1998, 14, 2670.
20. Kang, H. W.; Tabata, Y.; Ikada, Y. Biomaterials 1999, 20, 1339.
21. Monleòn Pradas, M.; Gòmez Ribelles, JL.; Serrano Aroca, A.; Gallego Ferrer, G.; Suay Antòn, J.; Pissis, P. Polymer 2001, 42, 4667.
22. Chen, J.; Park, K. J Controlled Release 2000, 65, 73.
23. Chen, J.; Blevins, W. E.; Park, H.; Park, K. J Controlled Release 2000, 64, 39.
24. Chen, J.; Park, K. Carbohydr Polym 2000, 41, 259.
25. Janata, J. Principles of Chemical Sensors; Plenum: New York, 1989.
26. Traiel, T.; Kost, J.; Smoder, A. Biotechnol Bioeng 2003, 84, 20.

27. Sudipto, N. R.; Johonson, A. R.; Crone, W. C.; Beebe, D. J. J Microelectromechanical Sys 2002, 11, 1.
28. Westman, L.; Lindstrom, T. J Appl Sci 1981, 26, 2561.
29. Chen, J.; Park, H.; Park, K. J Biomed Mater Res 1999, 44, 53.
30. Nakamoto, T.; Fukuda, A.; Moriizumi, T.; Asakura, Y. Sens Actuators B 1991, 3, 221.
31. Martin, S. J.; Granstaff, V. E.; Frye, G. C. Ricco, A. J. Using QCM for simultaneously sense mass accumulation and solution properties, Proc. Transducers '91, San Francisco, C. A.; USA, 1991, pp 785–788.
32. Faccio, M.; Ferri, G.; Mancini, F.; Di Rosa, P. Sens Actuators 1991, 32, 25.
33. Lambrechts, M.; Sansen, W. Biosensors: Microelectrochemical Devices; Institute of Physics Publishing: Bristol, UK, 1992.
34. Casilli, S.; Malitesta, C.; Conoci, P.; Petralia, S.; Sortino, S.; Valli, L. Biosens Actuators 2004, 1448, 1.
35. Sauerbrey, G. Z. J Phys 1959, 105, 206.
36. Esposito, F.; Del Nobile M. A.; Mensitieri G.; Nicolais, L. J Appl Polym Sci 1996, 60, 2403.
37. Sannino, A.; Mensitieri, G.; Del Nobile, M. A.; Capitani, D.; Segre, A. L. Macromolecules 2000, 33, 430.
38. Sannino, A. Ph.D. Thesis, University of Naples, 2000.
39. Martin, S. J.; Frye, G. F. IEEE Ultrasonics Symp Proc 1991, 1, 393.
40. Ballantine, D. S. Jr.; White, R. M.; Martin, S. J.; Ricco, A. J.; Frye, G. C.; Zellers, F. T.; Wohltjen, H. Acoustic Wave Sensors: Theory, Design and Physico-Chemical Applications; Academic Press: San Diego, 1997.
41. Moseley, P. T. Non-Nernstian, Potential-Generating Gas Sensors; Moseley, P. T.; Tofield, B. C., Eds. Adam Hilger: Bristol, 1987, p. 139.
42. Kanazawa, K. K.; Gordon, J. G. Anal Chem 1985, 57, 1770.
43. Martin, S. J.; Granstaff, V. E.; Frye, G. C.; Ricco, A. J. Using quartz crystal microbalance simultaneously sense mass accumulation and solution properties. Solid-State Sensors and Actuators 1991. Digest of Technical Papers, TRANS'91 International Conference on 1991, p 785.
44. Barnes, C. Sens Actuators A 1992, 30, 197.
45. Nomura, T.; Okuhara, M. Anal Chim Acta 1982, 142, 281.
46. Auge, J.; Hauptmann, P.; Eichelbaum, F.; Rosler, S. Sens Actuators B 1994, 18–19, 518.
47. Pan, W.; Durning, C. J.; Turro, N. J. Langmuir 1996, 12, 4469.
48. Sannino, A.; Nicolais, L. Polymer 2005, 46, 4676.
49. Sannino, A.; Esposito, A.; De Rosa, A.; Cozzolino, A.; Ambrosio, L.; Nicolais, L. J Biomed Mat Res A 2003, 67, 1016.
50. Sannino, A.; Netti, P. A.; Mensitieri, G.; Nicolais, L. Compos Sci Technol 2003, 63, 2411.